Evaluation of sonocatalytic degradation of phenol in the presence of zirconium oxide and cerium oxide nanocatalysts

F. Ghasemi[1], A. Naghizadeh[1,2*], G. A. M. Ali[3,4], V. K. Gupta[5*], Shilpi Agarwal[5], B. Mansouri[2]

[1] *Department of Environmental Health Engineering, Faculty of Health, Birjand University of Medical Science, Birjand, Iran*

[2] *Medical Toxicology and Drug Abuse Research Center (MTDRC), Birjand University of Medical Sciences, Birjand, Iran*

[3] *Chemistry Department, Faculty of Science, Al-Azhar University, Assiut 71524, Egypt*

[4] *The Smart Materials Research Institute, Southern Federal University, Sladkova Str. 178/24, Rostov-on-Don, Russian Federation*

[5] *Department of Biological Sciences, Faculty of Science, King Abdulaziz University, Jeddah, Saudi Arabia*

This study investigates the phenol sonocatalytic decomposition in the presence of zirconium oxide and cerium oxide nanoparticles. Different parameters, such as contact time, pH, phenol density, catalyst dose, and temperature on phenol degradation, were investigated. All experiments were performed at ultrasound frequency of 37 kHz. The results show that the maximum degradation of phenol in the presence of zirconium oxide and cerium oxide nanocatalysts was 23.64 and 19.01%, respectively. The optimum conditions were: phenol concentration 10 mg/L, time 30 min, pH 3, catalyst dosages 0.4 g/L, and temperature 30 °C. The findings recommend using both zirconium and cerium oxides as nanocatalysts for phenolic compounds degradation.

Keywords: Phenol, Zirconium oxide, Cerium oxide, Sonocatalysis.

INTRODUCTION

Water contamination with aromatic compounds such as dyes and phenols and their derivatives with a long half-life are sustainable in the environment and supposed to be a potential danger for humans and the environment [1-4]. These compounds exist in industrial wastes and are the main source of water pollution [5-8]. Phenol and its derivatives enter surface waters naturally through plants and algae decomposition and non-naturally through industrial wastewaters [9-11]. Phenol major pollutant sources include color manufacturing industries in a water environment, production of pesticides, gasoline, steel, oil and petrochemicals, leather, detergents, synthetic textiles, electronics, glass, explosives, cosmetics, and medical preparations [12-14]. Phenol compounds are considered priority pollutants due to their toxicity to the organism [15-17]. These compounds at low concentrations in drinking water can cause taste and odor changes [18]. In addition, they are toxic to aquatic plants and human life. Phenol and its derivatives are potentially carcinogenic. Swallowing phenols at a 10 to 240 mg/L concentration for a long time can cause mouth inflammation, diarrhea, dark urine, and visual problems. Toxic phenol concentration in blood is approximately in the range of 4.7 to 130 mg/L [19]. Exposure to excessive phenol can affect the brain, gastrointestinal system, eyes, heart, liver, lung, skin, kidney, and pancreas [20]. According to the World Health Organization recommendation, an acceptable concentration of phenol in drinking water is 1 μg/L [21]. The United States environmental protection agency determined allowable phenol levels in industrial wastewater discharged into the rivers as less than 0.1 mg/L [22].

Different methods were proposed for phenol removal, such as oxidation, photocatalytic degradation, biodegradation, chemical coagulation, solvent extraction, burning, reverse osmosis, microfiltration, ultrasonic irradiation, ozonation, and absorption [5, 14, 18, 23-30]. Nevertheless, these methods are increasingly limited due to the high cost. Moreover, such methods are non-destructive because they just transfer the organic compound from water to another phase, thus easily making secondary pollutions [31]. Using new approaches based on ultrasound waves with advanced oxidation processes is remarkable [32, 33]. Soundwave may have more advantages against other advanced practical treatment methods because of the accelerating decomposition of organic compounds that resist water. Practical advanced treatment methods need chemical materials and input energy to achieve an acceptable level for decomposition [34]. In the present method, under ultrasound wave performance, vapors and trapped gas in a liquid,

* To whom all correspondence should be sent:
E-mail: al.naghizadeh@yahoo.com
    vinodfcy@gmail.com

created by cavitation phenomena and through very high temperature, organic pollutants instantly decomposed directly or indirectly using hydroxyl radicals within collapsing cavitation bubbles [21, 35-37].

However, organic pollutants decomposition using ultrasound usually needs high energy and high reaction time [38]. To overcome this problem, the sonocatalytic destruction process was extended [39, 40]. The sonocatalytic method has high safety, simplicity, and efficiency [41]. The nanoparticles used in this study are zirconium oxide (ZrO_2) and cerium oxide (CeO_2). ZrO_2 nanoparticles are used as a catalyst because of their low price, non-toxicity, high chemical stability, hydrophilicity, catalyst activity, etc. [23, 42]. CeO_2 is another effective catalyst for organic materials oxidation, such as phenol and cyclohexane [43]. Several studies about phenol removal were conducted through sonocatalysis, but there is no publication related to phenol removal by sonocatalysis in the presence of CeO_2 and ZrO_2. Therefore, this study investigates the efficiency of CeO_2 and ZrO_2 nanoparticles as catalysts for phenol degradation through the sonocatalytic method.

MATERIAL AND METHOD

This practical study was performed experimentally on a laboratory scale. In this work, ZrO_2 and CeO_2 with 99.95 and 99.97% purity, respectively, were used as catalysts. At first, a stock solution (500 mg/L) was prepared by dissolving 0.5 g of phenol in 1000 mL of distilled water. The phenol removal experiments were performed in the presence of nanoparticles of ZrO_2 and CeO_2 in Erlenmayer flasks. The used frequency was 37 kHz, and the studied pH values were in the range of 2-11. After finding the optimal pH, the optimal dose of the catalyst was determined. Five dosages of catalyst (0.1, 0.2, 0.3, 0.4, 0.5 g/L) were examined. After determining the optimal pH and catalyst dosage, contact time (10, 20, 30, 40, 50 min) and initial phenol concentration (10, 20, 30, 40, 50 mg/L) were optimized. Finally, the experiments were performed at different temperatures (20, 30, 40, 50, and 60 °C), and the optimal temperature was found. In the different stages of research, phenol concentration was determined on a spectrophotometer at a wavelength of 500 nm. The structure and morphology of ZrO_2 and CeO_2 nanocatalysts were characterized using X-ray diffraction (XRD) and scanning electron microscopy (SEM).

RESULTS AND DISCUSSION
ZrO₂ and CeO₂ nanocatalysts characterization

XRD patterns and SEM images of ZrO_2 and CeO_2 nanoparticles are shown in Figs. 1 and 2, respectively.
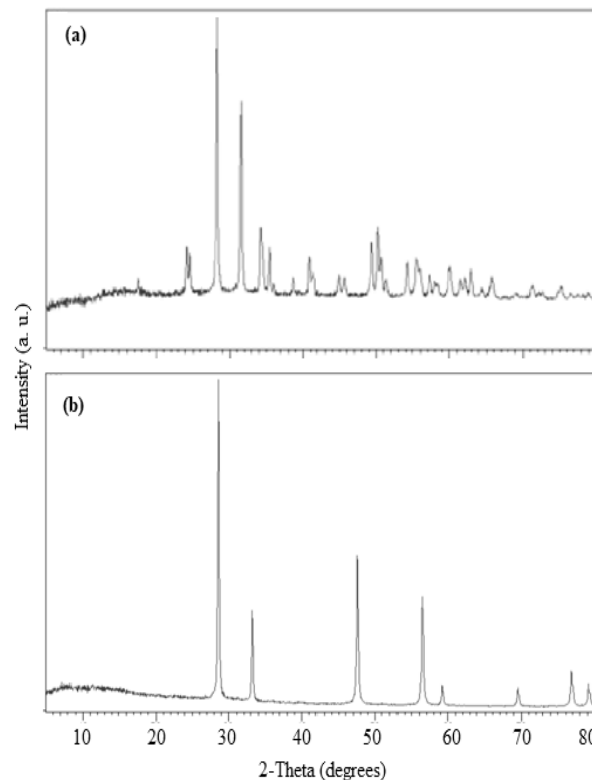

Fig. 1. X-ray diffraction patterns for ZrO_2 (a) and CeO_2 (b).

XRD is a technique that is used widely for determining structural specifications. SEM is used for investigating surface specifications and nanoparticle shape. In the two patterns, the number of peaks and the number of diffraction angles are different which shows a unique and completely different crystalline structure. ZrO_2 and CeO_2 XRD patterns are shown in Figs. 1a and 1b, respectively. Peaks related to ZrO_2 are located at 24.14, 28.27, 31.56, 34.25, 34.50, 40.83, 49.34 and 50.21°. For CeO_2, the peaks are located at 28.64, 33.17, 47.56, 56.41, 59.16, 69.49, 76.73, and 79.15°, which shows the tetragonal and cubic property of these nanoparticles [23, 44, 45]. Data on particle size (Ps), obtained based on peaks width, show that ZrO_2 size is smaller than that of CeO_2 (38 and 46 nm for ZrO_2 and CeO_2, respectively) using the Scherrer equation ($Ps=k\lambda/\beta cos\theta$, where k = 0.9, λ is the Cu-target wavelength, β is the full-width at half-maximum of the diffraction peak, and θ is the diffraction angle [46-48].
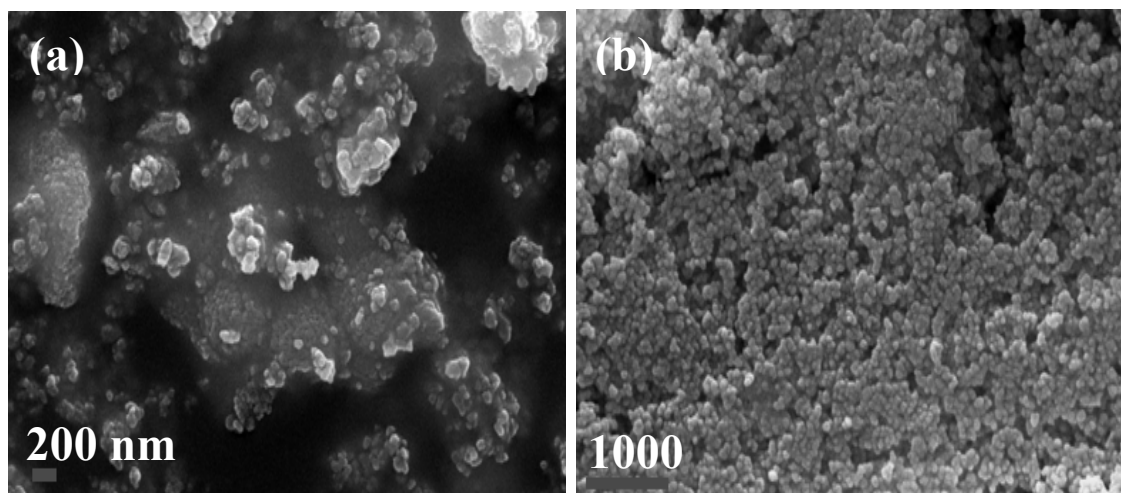
Fig. 2. SEM images of ZrO_2 (a) and CeO_2 (b).

CeO_2 nanoparticles are light yellow, of spherical shape, and the density is equal to 7.132 g/cm^3, while ZrO_2 nanoparticles are white, of approximately spherical shape with a density of 5.890 g/cm^3, as can be seen from Fig. 2. The smaller spherical particles of ZrO_2 (Fig. 2a) are widely distributed, providing a larger amount of active centers.

Effect of pH on phenol degradation by sonocatalytic process

In this study, the amount of phenol removal in the pH range from 2 to 11 was investigated in the presence of ZrO_2 and CeO_2 nanoparticles. As displayed in Fig. 3, the maximum amount of phenol removal by a sonocatalytic process using ultrasound (US) only and in the presence of ZrO_2 and CeO_2 is at pH 3. The removal ratio was 14.6, 13.73, and 0.38% using ZrO_2, CeO_2, and US, respectively. pH has an essential effect on phenol destruction.
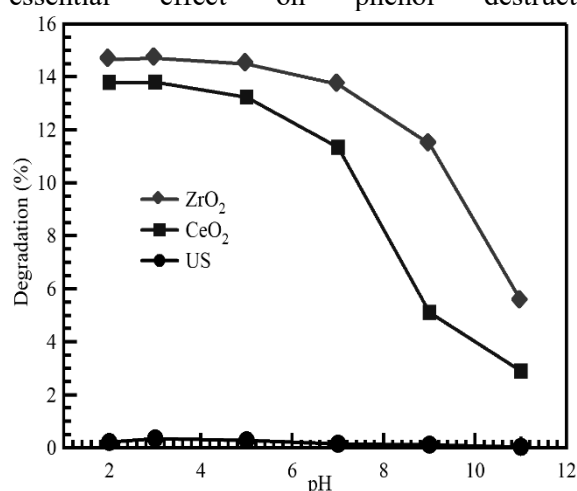

Fig. 3. pH effect on phenol removal by nanocatalytic process in the presence of ZrO_2 and CeO_2 nanoparticles.

Phenol adsorption and catalyst surface charge will vary with changes in the pH value. This factor affects the interpretation of removing pollutants through the sonocatalytic method because of different functions of surface ionization, hydroxyl radical formation, particle aggregation, and pollutant specifications, which can affect catalyst adsorption and congestion [49]. It is known that the degradation reactions can be accelerated under acidic conditions while under strongly alkaline conditions; due to the repulsion force from the negatively charged surface, phenol anions in aqueous solution are mainly degraded through radical (OH) oxidation, which is a slow-motion degradation process [5]. When catalysts are released in the water environment, they have a tendency to accumulate, which leads to an increase in catalyst dispersion in the acidic environment due to the repulsion between catalyst surfaces. Also, in an acidic environment, hydroxyl radical production increases, which leads to stronger decomposition of the nanocatalysts [50]. In alkaline conditions, the generated phenol ions are concentrated between water and gas and cannot enter the cavitation bubbles, and they react with OH⁻ radicals outside the cavitation bubbles; hence the rate of degradation is lower [51]. These results agree with those reported by MacManamon *et al.* about phenol photocatalytic decomposition in the presence of TiO_2 and ZrO_2, which showed a stronger phenol removal in the acidic environment [52, 53].

Effect of initial dose on phenol degradation by sonocatalytic process

Fig. 4 shows the removal percentage of phenol at different concentrations and different times in the presence of ZrO_2 and CeO_2.
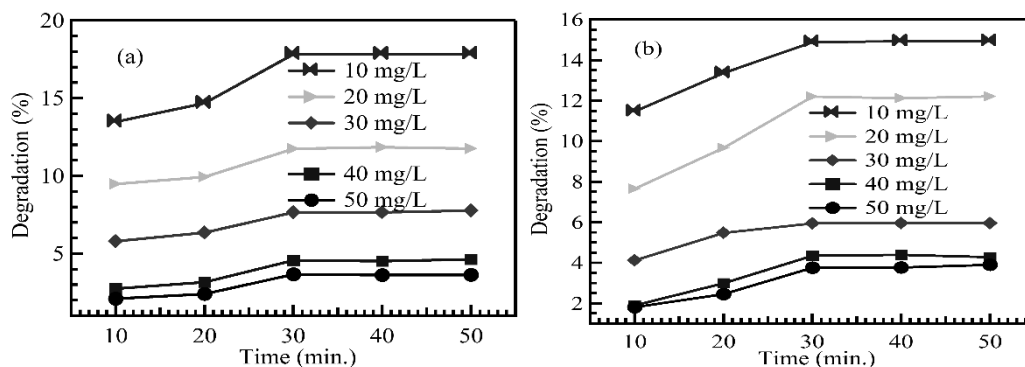
Fig. 4. Effect of time on phenol removal by sonocatalytic process in the presence of ZrO₂ (a) and CeO₂ (b) nanoparticles.

The phenol removal percentage reaches a maximum in 30 min, and at 10 mg/L concentration, which equals 17.77% and 14.98%, respectively. After this time, the removal is constant. With regard to Fig. 4, phenol removal amounts of 10, 20, 30, 40, 50 mg/L after 30 min, equal to 14.98, 12.23, 6.06, 4.30, and 3.88%, respectively. As observed, phenol removal percentage until 30 min, for all concentrations increases, and there is no increment beyond this time. In Fig. 4, phenol removal amounts at 10, 20, 30, 40, 50 mg/L concentrations after 30 min equal to 17.77, 11.71, 7.77, 4.58, and 3.64%, respectively. Also, in Fig. 4, after 30 min, the phenol removal reaches a constant value. The reason for decreasing decomposition efficiency with increasing primary concentration can be explained as follows: at the same nanoparticles concentration, constant time, and pH, the hydroxyl free radical density in solution is equal, therefore phenol reaction with OH⁻ radicals at low concentration increases and leads to increasing phenol decomposition by free radicals [50]. In addition, when phenol concentration increases in the liquid phase, it may increase the partial pressure in cavitation bubbles, and finally, the decreased solvent temperature can be effective for dissolution. Another reason for these phenomena is that comparing with lower phenol concentration, fewer sound waves in the solution can destruct these molecules because produced sound waves are constant at different concentrations. Finally, sound waves do not reach the fundamental particle's surface, and this factor causes decreasing oxidation. It can be seen that with increasing contact time, removal amount increases and then reaches a plateau. The most important reason for this phenomenon can be that with passing the time, more hydroxyl free radicals are produced, which are spent for phenol molecules oxidation, and as a result, phenol concentration decreases, moreover in primary moments, pollutant concentration is high, and it is possible that more collusions between phenol molecules and hydroxyl free radicals occur.

With time passing, the concentration of pollutants decreases, and the existing hydroxyl free radicals are spent on phenol metabolites oxidation, which causes slowing down of the removal amount.

From these data, we can conclude that the sonocatalytic process is more efficient in phenol removal in the presence of CeO₂ and ZrO₂ nanoparticles. In the study of Mahvi *et al.* performed in 2015 on tetracycline removal by chemical sonoprocess they concluded that the percentage of removed tetracycline increases [50]. A study conducted by McManamon *et al.* on phenol removal by photocatalysis process showed that up to 25 mg/L concentration, phenol removal increased, but after that decreased [52]. Research performed by Khataee *et al.* in 2015 on color removal by the sonocatalytic method revealed that with increasing color concentration, color removal decreased [54]. Another study performed by Hamdaouui *et al.* using the sonochemical method for removing tetra-chlorophenol showed that the efficiency decreased with increasing pollutant concentration [55]. Chowdhury *et al.* also reported in their study in 2009 about the sonochemical decomposition of organic compounds in which, with increasing concentration of organic compounds, removal efficiency decreased [56].

Effect of catalyst dose on phenol degradation by sonocatalytic process

As shown in Fig. 5 phenol removal efficiency with increasing CeO₂ nanoparticles and ZrO₂ particles dose increases from 0.1 to 0.4 g/L and then is constant. The maximum percentage of phenol removal is in a 0.4 g/L catalyst for CeO₂ and ZrO₂ nanoparticles, 19.0 and 23.6%, respectively.
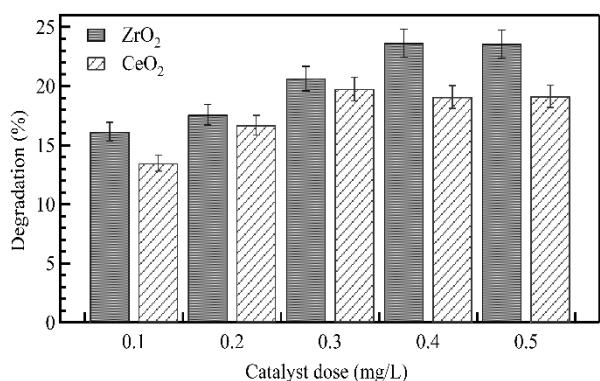
Fig. 5. Catalyst dose effect on phenol removal by sonocatalytic process in the presence of ZrO_2 and CeO_2.

This can be attributed to the fact that when all phenol molecules are sitting on the catalyst, adding more catalyst, because of the absence of phenol molecules does not affect removal efficiency [50]. Increasing phenol removal by increased catalyst dose can be stated because of increasing active sites, and more hydroxyl radicals produced [54]. As specified, with increasing catalyst dose from 0.4 g/L, the amount of removal phenol remained constant because of decreasing ultrasound waves to nanoparticles, this action leads to catalyst aggregation, and finally, available and active sites decreased [20, 57]. Babuponnumsami *et al.* studied the phenol removal and showed that phenol removal up to 0.5 g/L of zero-valent iron nanoparticles increased [58]. Bansal *et al.* also reported increasing color removal with increasing the amount of ZrO_2 nanoparticles [23].

Effect of temperature on phenol degradation by sonocatalytic process

Fig. 6 shows the temperature effect on phenol removal by sonocatalytic process in the presence of ZrO_2 and CeO_2 nanoparticles. Unlike the current reaction system, the rate of sonochemical reactions decreases by increasing the solution temperature beyond a certain limit. Due to the effects of cavitation, increasing the temperature to reach the desired level increases covariance activity due to sufficient energy generation. Subsequently, it increases the number of cavity bubbles in sonocatalysis, resulting in an increase in the production of radicals and the degradation of pollutants. A higher temperature increase (higher than optimal) causes a higher solvent vapor pressure inside the cavitation bubbles filled with water vapor and leads to increased resistance to movement within the bubble during the collapse of cavitation cavities and cavitation energy dissipates [59, 60].
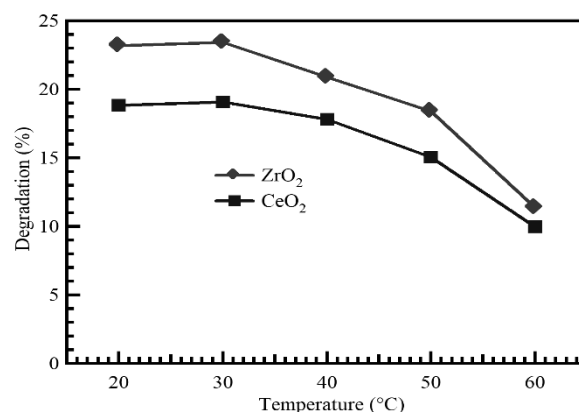

Fig. 6. Investigation of temperature effect on sonocatalytic phenol removal in the presence of ZrO_2 and CeO_2.

In this study, the amount of phenol sonocatalytic destruction at 20, 30, 40, 50, and 60 °C was investigated, and we can see that increasing temperature does not create a notable difference in phenol removal slightly increased up to 30 °C and then decreased. The increase occurred because of increasing reaction speed and, on the other hand, in this process, increasing water vapor leads to decreasing sonocatalysis activity and finally decreasing phenol removal [61]. Combining these two actions makes very little increase in phenol removal. Golash *et al.* on ultrasonic analysis of sewage showed an increase in decomposition rates up to 25 °C followed by a decrease [62]. Also, the results of the study by Barik *et al.* on the degradation of 2,4-dichlorophenol showed the temperature of 34 °C as optimal for decomposition [59].

Comparison of the activity of various processes in phenol removal

Under optimal conditions, phenol removal was performed in the presence of ultrasound waves, and the efficiency of its removal by CeO_2 and ZrO_2 nanoparticles was determined and compared with that of the sonocatalysis process. As shown in Fig. 7, the amount of phenol removal in the presence of ultrasound waves is very low (0.68%) while the amounts of phenol removal in the presence of CeO_2 and ZrO_2 nanoparticles were 4.79 and 9.41%, respectively. This value for the sonocatalytic process using ultrasound in the presence of CeO_2 and ZrO_2 equals 19.01 and 23.64%, respectively. The decomposition of organic pollutants by ultrasound usually needs high energy and high reaction duration time [38].
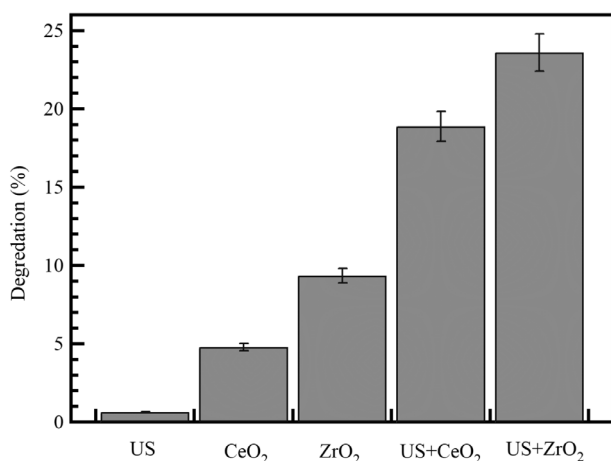
Fig. 7. Comparing phenol removal in the different processes.

The reasons behind the higher catalytic activity of ZrO_2 than CeO_2 are the wider bandgap (5 and 3.1 eV, for ZrO_2 and CeO_2, respectively) and higher stability [63, 64]. In addition, larger amounts of active centers are available on the smaller particle size of ZrO_2 than CeO_2 (38 and 46 nm, respectively).

Only sonowaves cannot decompose phenol to a stable compound; therefore, we can add a catalyst to increase phenol removal efficiency [65]. In the study of Yehia *et al.* on phenol removal by a Fenton-process in the presence of ultrasound it was reported that the amount of phenol removed in the presence of ultrasound waves in 60 min is 20% (less than the Fenton-process) [5].

CONCLUSIONS

ZrO_2 and CeO_2 nanocatalysts show tetragonal and cubic structures with particle size of 38 and 46 nm, respectively. ZrO_2 and CeO_2 nanocatalysts show an excellent catalytic performance for phenol degradation using the sonocatalytic method. The optimum conditions were: phenol concentration 10 mg/L, time 30 min, pH 3, catalyst dosages 0.4 g/L, and temperature 30 °C. The maximum amounts of phenol removal using ZrO_2 and CeO_2 were 23.63 and 19.01%, respectively. According to these research results, ZrO_2 has a higher potential than CeO_2 as a catalyst for phenol decomposition using the sonocatalytic method. The findings recommend using both zirconium and cerium oxides as nanocatalysts for phenolic compounds degradation.

REFERENCES

1. H. H. Abdel Ghafar, G. A. M. Ali, O. A. Fouad, S. A. Makhlouf, *Desalin. Water Treat.*, **53**(11), 2980 (2015).
2. V. K. Gupta, S. Agarwal, H. Sadegh, G. A. M. Ali, A. K. Bharti, A. S. Hamdy, *J. Mol. Liq.*, **237**, 466 (2017).
3. S. Agarwal, H. Sadegh, Monajjemi Majid, A. S. H. Makhlouf, G. A. M. Ali, A. O. H. Memar, R. Shahryari-ghoshekandi, I. Tyagi, V.K. Gupta, *J. Mol. Liq.*, **218**, 191 (2016).
4. I. Fatimah, R. Nurillahi, I. Sahroni, G. Fadillah, B.H. Nugroho, A. Kamari, O. Muraza, *Journal of Water Process Engineering*, **37**, 101418 (2020).
5. F. Z. Yehia, G. Eshaq, A. M. Rabie, A. H. Mady, A. E. ElMetwally, *Egypt. J. Pet.*, **24**(1), 13 (2015).
6. S. M. Seyed Arabi, R. S. Lalehloo, M. R. T. B. Olyai, G. A. M. Ali, H. Sadegh, *Physica E*, **106**, 150 (2019).
7. Y. L. Qi, G. Han, X. C. Song, *Mater. Res. Bull.*, **102**, 16 (2018).
8. M. Solehudin, U. Sirimahachai, G. A. M. Ali, K. F. Chong, S. Wongnawa, *Adv. Powder Technol.*, **31**(5), 1891 (2020).
9. S. Yapar, V. Ozbudak, A. Dias, A. Lopes, *J. Hazard. Mater.*, **121**(1-3), 135 (2005).
10. D. G. Aseev, M. R. Sizykh, A. A. Batoeva, *Russ. J. Phys. Chem. A*, **91**(12), 2331 (2017).
11. G. Eshaq, S. Wang, H. Sun, M. Sillanpää, *Sep. Purif. Technol.*, **231**, 115915 (2020).
12. M. Ahmaruzzaman, *Adv. Colloid Interface Sci.*, **143**(1-2), 48 (2008).
13. S.-H. Lin, R.-S. Juang, *Journal of Environmental Management*, **90**(3), 1336 (2009).
14. M. Kilic, E. Apaydin-Varol, A. E. Pütün, *J. Hazard. Mater.*, **189**(1-2), 397 (2011).
15. R. I. Yousef, B. El-Eswed, A. a. H. Al-Muhtaseb, *Chem. Eng. J.*, **171**(3), 1143 (2011).
16. S. Yao, Y. Zhang, Z. Shi, S. Wang, *Russ. J. Phys. Chem. A*, **87**(1), 69 (2013).
17. G. Eshaq, S. Wang, H. Sun, M. Sillanpaa, *J. Hazard. Mater.*, **382**, 121059 (2020).
18. N. N. M. Zain, N. K. Abu Bakar, S. Mohamad, N. M. Saleh, *Spectrochim. Acta, Part A*, **118**, 1121 (2014).
19. I. Z. Shirgaonkar, H. S. Joglekar, V. D. Mundale, J. B. Joshi, *J. Chem. Eng. Data*, **37**(2), 175 (1992).
20. Q. Jia, A. C. Lua, *J. Anal. Appl. Pyrolysis*, **83**(2), 175 (2008).
21. P. Singh, Sonu, P. Raizada, A. Sudhaik, P. Shandilya, P. Thakur, S. Agarwal, V. K. Gupta, *J. Saudi Chem. Soc.*, doi.org/10.1016 j.jscs.2018.10.005 (2018).
22. H. B. Senturk, D. Ozdes, A. Gundogdu, C. Duran, M. Soylak, *J. Hazard. Mater.*, **172**(1), 353 (2009).
23. P. Bansal, G.R. Chaudhary, S.K. Mehta, *Chem. Eng. J.*, **280**, 475 (2015).
24. L. Svoboda, P. Praus, M. J. Lima, M. J. Sampaio, D. Matýsek, M. Ritz, R. Dvorský, J. L. Faria, C. G. Silva, *Mater. Res. Bull.*, **100**, 322 (2018).
25. Y. Li, Q. Du, T. Liu, J. Sun, Y. Jiao, Y. Xia, L. Xia, Z. Wang, W. Zhang, K. Wang, H. Zhu, D. Wu, *Mater. Res. Bull.*, **47**(8), 1898 (2012).

26. A. M. Asiri, M. S. Al-Amoudi, T. A. Al-Talhi, A. D. Al-Talhi, *J. Saudi Chem. Soc.*, **15**(2), 121 (2011).
27. H. Bashiri, M. Rafiee, *J. Saudi Chem. Soc.*, **20**(4), 474 (2016).
28. W.-M. Liu, *Chem. Res. Chin. Univ.*, **29**(2), 314 (2013).
29. A. S. Ethiraj, P. Uttam, V. K, K. F. Chong, G. A. M. Ali, *Mater. Chem. Phys.*, **31**(5), 1891 (2020).
30. A. Sharifi, L. Montazerghaem, A. Naeimi, A. R. Abhari, M. Vafaee, G. A. M. Ali, H. Sadegh, *Journal of Environmental Management*, **247**, 624 (2019).
31. J. Wang, Y. Jiang, Z. Zhang, G. Zhao, G. Zhang, T. Ma, W. Sun, *Desalination*, **216**(1-3), 196 (2007).
32. M. Papadaki, *Sep. Purif. Technol.*, **34**(1-3), 35 (2004).
33. F. Hayati, A. A. Isari, B. Anvaripour, M. Fattahi, B. Kakavandi, *Chem. Eng. J.*, **381**, 122636 (2020).
34. N. H. Ince, G. Tezcanli, R. K. Belen, İ. G. Apikyan, *Appl. Catal., B*, **29**(3), 167 (2001).
35. K. S. Suslick, S. J. Doktycz, E. B. Flint, *Ultrasonics*, **28**(5), 280 (1990).
36. M. Sivakumar, A. B. Pandit, *Ultrason. Sonochem.*, **8**(3), 233 (2001).
37. B. Nanzai, K. Okitsu, N. Takenaka, H. Bandow, Y. Maeda, *Ultrason. Sonochem.*, **15**(4), 478 (2008).
38. M. T. Taghizadeh, A. Mehrdad, *Ultrason. Sonochem.*, **10**(6), 309 (2003).
39. M. Kubo, K. Matsuoka, A. Takahashi, N. Shibasaki-Kitakawa, T. Yonemoto, *Ultrason. Sonochem.*, **12**(4), 263 (2005).
40. J. Wang, Z. Pan, Z. Zhang, X. Zhang, F. Wen, T. Ma, Y. Jiang, L. Wang, L. Xu, P. Kang, *Ultrason. Sonochem.*, **13**(6), 493 (2006).
41. J. Wang, B. Guo, X. Zhang, Z. Zhang, J. Han, J. Wu, *Ultrason. Sonochem.*, **12**(5), 331 (2005).
42. X. Yu, W.-C. Zhu, S. Gao, L.-l. Chen, H.-J. Yuan, J.-H. Luo, Z.-l. Wang, W.-X. Zhang, *Chem. Res. Chin. Univ.*, **29**(5), 986 (2013).
43. H. Zhao, G. Zhang, Q. Zhang, *Ultrason. Sonochem.*, **21**(3), 991 (2014).
44. S. Lu, K. Li, F. Huang, C. Chen, B. Sun, *Appl. Surf. Sci.*, **400**, 277 (2017).
45. N. C. S. Selvam, A. Manikandan, L. J. Kennedy, J. J. Vijaya, *J. Colloid Interface Sci.*, **389**(1), 91 (2013).
46. A. Patterson, *Physical Review*, **56**(10), 978 (1939).
47. O. A. Fouad, S. A. Makhlouf, G. A. M. Ali, A. Y. El-Sayed, *Mater. Chem. Phys.*, **128**(1), 70 (2011).
48. O. A. Fouad, G. A. M. Ali, M. A. I. El-Erian, S. A. Makhlouf, *Nano*, **7**(5), 1250038 (2012).
49. N. Ghows, M. H. Entezari, *J. Hazard. Mater.*, **195**, 132 (2011).
50. M. Hoseini, G. H. Safari, H. Kamani, J. Jaafari, A. Mahvi, *Iran. J. Health Environ.*, **8**(2), 141 (2015).
51. K. P. Jyothi, S. Yesodharan, E.P. Yesodharan, *Ultrason. Sonochem.*, **21**(5), 1787 (2014).
52. C. McManamon, J. D. Holmes, M. A. Morris, *J. Hazard. Mater.*, **193**, 120 (2011).
53. M. Giahi, D. Pathania, S. Agarwal, G.A.M. Ali, K.F. Chong, V.K. Gupta, *Studia Universitatis Babes-Bolyai, Chemia*, **64**(1), 7 (2019).
54. A. Khataee, M. Sheydaei, A. Hassani, M. Taseidifar, S. Karaca, *Ultrason. Sonochem.*, **22**, 404 (2015).
55. O. Hamdaoui, E. Naffrechoux, *Ultrason. Sonochem.*, **15**(6), 981 (2008).
56. P. Chowdhury, T. Viraraghavan, *Sci. Total Environ.*, **407**(8), 2474 (2009).
57. S. G. Anju, S. Yesodharan, E. P. Yesodharan, *Chem. Eng. J.*, **189-190**, 84 (2012).
58. A. Babuponnusami, K. Muthukumar, *Sep. Purif. Technol.*, **98**, 130 (2012).
59. A. J. Barik, P. R. Gogate, *Ultrason. Sonochem.*, **36**, 517 (2017).
60. M. Chiha, O. Hamdaoui, S. Baup, N. Gondrexon, *Ultrason. Sonochem.*, **18**(5), 943 (2011).
61. J. Wang, Z. Jiang, Z. Zhang, Y. Xie, Y. Lv, J. Li, Y. Deng, X. Zhang, *Sep. Purif. Technol.*, **67**(1), 38 (2009).
62. N. Golash, P. R. Gogate, *Ultrason. Sonochem.*, **19**(5), 1051 (2012).
63. J. Wang, Y. Lv, L. Zhang, B. Liu, R. Jiang, G. Han, R. Xu, X. Zhang, *Ultrason. Sonochem.*, **17**(4), 642 (2010).
64. Y. Kristianto, R. Saleh, Effect of CeO_2 promotion on the sonocatalytic performance of ZrO_2 nanoparticle catalysts, AIP Conf. Proc., AIP Publishing LLC, 2018, p. 020042.
65. M. H. Entezari, C. Pétrier, P. Devidal, *Ultrason. Sonochem.*, **10**(2), 103 (2003).